Atmospheric
Chemistry
and Physics
Discussions

Lower tropospheric ozone over the North China Plain: variability and trends revealed by IASI satellite observations for 2008-2016

Gaëlle Dufour[1], Maxim Eremenko[1], Matthias Beekmann[1], Juan Cuesta[1], Gilles Foret[1], Weili Lin[2], Yi Liu[3], Xiaobin Xu[4], Yuli Zhang[3]

[1] Laboratoire Inter-universitaire des Systèmes Atmosphériques (LISA), UMR7583, Universités Paris-Est Créteil et Paris Diderot, CNRS, Créteil, France
[2] Meteorological Observation Center, China Meteorological Administration, Beijing, China
[3] Institute of Atmospheric Physics, Chinese Academy of Sciences, Beijing, China
[4] Key Laboratory for Atmospheric Chemistry of China Meteorological Administration, Chinese Academy of Meteorological Sciences, Beijing, China

Correspondence to: Gaëlle Dufour (gaelle.dufour@lisa.u-pec.fr)

Abstract.

China, and especially the North China Plain (NCP), is a highly polluted region. Emission reductions have been applied since about 10 years, starting with SO_2 emissions in 2006 and with NO_x emissions in 2010. Recent studies show a decrease of NO_2 tropospheric column since 2013 and attributed to the NO_x emissions reduction. Quantifying how these emission reductions translates to the ozone concentrations remains. In this study, we use the lower tropospheric (LT) columns (surface-6km asl) derived from the IASI satellite instrument to describe the variability and trend of LT ozone over the NCP for 2008-2016. Deseasonalized monthly timeseries show two distinct periods: a first period (2008-2012) with no significant trend (< -0.1 %/yr) and a second period (2013-2016) with a highly significant negative trend of -1.2 %/yr, leading to an overall trend of -0.77 %/yr for 2008-2016. We explore the dynamical and chemical factors that could explain this overall negative trend using a multivariate regression model. The results suggest that the negative trend observed from IASI could arise from a reduction of the stratosphere-to-troposphere transport combined with reduction of regional precursor emissions, as suggested by the used CO proxy. However, no negative trend has been reported from background surface measurements in this Chinese region. As well, recent work made within the framework of the TOAR (Tropospheric Ozone Assessment Report) initiative reveals discrepancies in the sign of the trends of tropospheric ozone derived from infrared and ultraviolet satellite instruments, with no conclusive explanation found until now. We then investigate the IASI retrieval stability and robustness and compare it with surface and ozonesonde measurements and the independent IASI instrument aboard the Metop-B satellite. One issue that arises from the different comparison concerns the impact of the sampling differences between the different datasets on the different calculated trends.

1 Introduction

The rapid economic development and urbanization in China during the last three decades resulted in rising pollutant

Atmospheric
Chemistry
and Physics
Discussions

emissions leading to the largest pollutant concentrations in the world, largely exceeding the recommended outdoor air pollutant thresholds from the World Health Organization (WHO) for the major pollutants (ozone, $PM_{2.5}$, and PM_{10}). Several studies point toward a general ozone (O_3) increase over some parts of China mainly attributed to the emission rising, as well at the surface (Cooper et al., 2014; Ma et al., 2016; Wang et al., 2009), as in the lower troposphere (Ding et al., 2008; Sun et

5 al., 2016; Wang et al., 2017b), or in the entire troposphere (Chen et al., 2015; Verstraeten et al., 2015; Wang et al., 2012; Xu and Lin, 2011). Only a few long-term O_3 measurements are available in China. Wang et al. (2009) reported an increase of surface O_3 of 0.58 ppb/yr during 1994-2007 at a regional station in Hong Kong. Ding et al. (2008) derived an O_3 trend of 2%/yr between 1995 and 2005 in the lower troposphere from the MOZAIC commercial aircraft measurements. Xu and Lin (2011) analyzed tropospheric ozone trends from satellite using the TOR (tropospheric ozone residual) approach during 1979-

10 2005 and found a trend of 1.10 DU per decade in summer over the North China Plain (NCP). More recently, Xu et al. (2016, 2018) reported on trends derived from surface measurements operated at Mt. Waliguan, on the Tibetan Plateau over the period 1994-2013. The derived general trend is about 0.1-0.3 ppbv/yr, with a more significant trend during spring and autumn, much smaller trend in winter and no significant trend in summer. Several studies are available on shorter time periods and for more recent years. In Beijing, Tang et al. (2009) reported on ozone trends of 1.1ppb/yr for the 2001-2006

15 period. Ma et al. (2016) and Sun et al. (2016) found significant increase of surface ozone at two stations representative of the NCP for the 2003-2015 period. Their analyses showed a trend of 1.13 ppb/yr at Shangdianzi and a trend of 2.1 ppb/yr during summertime at Mt. Tai, respectively. Verstraeten et al. (2015) show, using TES satellite observations, that tropospheric ozone over China has increased by about 7% between 2005 and 2010, increase attributed to the rise in Chinese emissions and to an increase in the downward transport of stratospheric ozone (Neu et al., 2014). Most of the long-term trends are

20 attributed to the large increase of precursor emissions, such as the NOx emissions, which have tripled since 1990 (e.g. Lin et al., 2017; Richter et al., 2005). However, ozone concentrations are also influenced by other factors, in particular dynamical factors, which drive most of the variability of ozone (e.g. Wespes et al., 2017b) with potential modulations of the trends. Among the processes impacting ozone concentrations, stratosphere-to-troposphere transport that brings ozone-rich air down to the surface in some cases (e.g. Dufour et al., 2010, 2015; Lin et al., 2015; Verstraeten et al., 2015) is one key parameter as

25 well as the processes, which modify the large-scale atmospheric circulation such as the El Nino-Southern Oscillation (ENSO), the quasi-biennial oscillation (QBO), the solar cycle (e.g. Ebojie et al., 2016; Oman et al., 2013; Wespes et al., 2016, 2017b). Facing the large pollutant increase since the 90s, China has started implementing stringent air quality controls starting in 2006 with reductions of SO_2 emissions and followed by successful emission reductions of NO_x more recently (e.g. van der A et al., 2017; Li et al., 2017; Ma et al., 2016). Only few studies evaluate the recent trends of ozone concentrations

30 for period encompassing the recent changes in NO_x emissions. Ma et al. (2016) used ozone data collected at the Shangdianzi background station, representative of the NCP to derive trends over 2003-2015. They did not find any significant correlation between ozone and NO_2 trends. They state that the changes of VOC emissions and the ratio VOC/NO_x might play a more important role in the observed increase of ozone than the reduced NO titration induced by NO_x emission reductions in agreement with conclusions of Sun et al. (2016) based on measurement at the Mt. Tai station. Indeed, VOC emissions had

continuously increased over 2000-2015 (Li et al., 2017). A very recent work done in the framework of the Tropospheric Ozone Assessment Report supported by the IGAC (International Global Atmospheric Chemistry) community states that ozone is generally increasing at the global scale over the recent decade. However, some inconsistencies between trends derived from infrared (IR) sounders like IASI and ultraviolet (UV) sounders like OMI with IR sounders showing negative

5 trends and UV sounders positive trends (Gaudel et al., 2018). A particular attention on the instrumental and retrieval stability has then to be paid when using satellite observations to derived tropospheric ozone trends.

In this study, we focus our analysis over the lower troposphere (LT) of the NCP using the thermal infrared IASI satellite observation for 2008-2016. We analyze the variability and recent trend (2008-2016) of the LT ozone columns in regards of different dynamical factors as well as proxies for emissions, such as carbon monoxide columns. Section 2 describes the IASI

10 ozone observations. Section 3 provides an analysis of the variability and trends of LT ozone over the NCP over 9 years (2008-2016) based on the IASI instrument onboard the Metop-A satellite, in flight since 2006. Section 4 evaluates the instrumental and retrieval stability of IASI and discusses the reliability of the IASI derived trends. Conclusions are given in Section 5.

2 IASI ozone observations

15 ### 2.1 IASI-A and IASI-B on the Metop platforms

The IASI (Infrared Atmospheric Sounding Interferometer) (Clerbaux et al., 2009) instruments are nadir-viewing Fourier transform spectrometers. They have been planned for flying on board the EUMETSAT (European Organisation for the Exploitation of Meteorological Satellites) Metop satellite. Currently, two versions of the instrument are in flight: one aboard the Metop-A platform since October 2006 and the Metop-B platform since September 2012. The IASI instruments operate in

20 the thermal infrared between 645 and 2760 cm^{-1} with an apodized resolution of 0.5 cm^{-1}. The field of view of the instrument is composed of a 2×2 matrix of pixels with a diameter at nadir of 12 km each. IASI scans the atmosphere with a swath width of 2200 km and crosses the equator at two fixed local solar times 9:30 am (descending mode) and 9:30 pm (ascending mode), allowing the monitoring of atmospheric composition twice a day at any location. The two Metop satellites are on the same orbit shifted by 180° leading to a time difference of about 50 minutes between the two IASI instruments (Boynard et

25 al., 2018).

2.2 IASI-LISA-O$_3$ retrieval

Ozone profiles are retrieved from the IASI radiances following the method described in Eremenko et al. (2008) and Dufour et al. (2012, 2015). The retrieval algorithm is based on the KOPRA radiative transfer model and its inversion tool (KOPRAFIT). A constrained least squares fit method with an analytical altitude-dependent regularization is used. The

30 regularization matrix is a combination of first order Tikhonov constraints (Tikhonov, 1963) with altitude-dependent coefficients (Kulawik et al., 2006). The coefficients are optimized both to maximize the degrees of freedom (DOF) of the

retrieval and to minimize the total error on the retrieved profile. Different a priori and constraints are used depending on the tropopause height, which is calculated from the temperature profile retrieved from IASI using the definition based on the lapse rate criterion (WMO, 1957). Three situations are considered: polar (<10 km), midlatitudes (10-14 km), and tropical (>14km). The a priori profiles are compiled from the ozonesonde climatology of McPeters et al. (2007). As shown in Dufour

5   et al. (2010, 2012), two semi-independent partial columns of ozone between the surface and 12 km can be considered: the lower-tropospheric column integrating the ozone profile from the surface to 6 km altitude – above sea level (asl) – and the upper-tropospheric column integrating the ozone profile from 6 to 12 km altitude. Note that the latter column can include stratospheric air masses depending on the tropopause height. The averaging kernels give information on the vertical sensitivity and resolution of the retrieval. The lower tropospheric column shows a maximum sensitivity typically between 3

10 and 4 km with a limited sensitivity to the surface (Dufour et al., 2012). From the retrieved profiles, different ozone partial columns can be calculated. The lower tropospheric column (LT) from the surface up to 6 km (asl) is considered in this study. Note that only the morning overpasses of IASI are considered for this study in order to remain in thermal conditions with a better sensitivity to the lower troposphere.

Recent studies based on IASI observations, mainly ammonia, reported on changes in the temperature product delivered by

15 EUMETSAT that impact the retrieval. The changes are related to different versions of the product (Van Damme et al., 2017). In order to avoid the potential impact of versioning of the auxiliary parameters (such as temperature profile, clouds screening, etc) on the ozone retrieval, we apply a self-consistent procedure. Surface temperature and temperature profiles are retrieved before the ozone retrieval. A data screening procedure is applied to filter cloudy scenes and to insure the data quality (Dufour et al., 2010, 2012; Eremenko et al., 2008).

20 **3 Variability and trends of LT ozone over the NCP**

3.1 Timeseries analysis method

The IASI observations are analyzed over a nine-year period (2008-2016) for IASI-A, the first instrument aboard Metop-A satellite and over a four-year period (2013-2016) for IASI-B, the second instrument aboard the Metop-B satellite. Each pixel is retrieved individually and filtered following the procedure previously described. Gridded monthly averages are computed

25 on a 0.25°x0.25° resolution grid from daily averages computed on the same grid for the East Asia domain (20-48°N, 100-150°E). As the principal focus of this study is the North China Plain, we then calculate regional averages from the gridded monthly means for this region in order to have regional monthly timeseries. The domain considered for the NCP ranges between 35°N and 41°N in latitude and between 114°E and 122°E in longitude (Fig. 1). Seasonal and annual timeseries are derived from the regional monthly timeseries. We also calculate the deseasonalized monthly timeseries. We use the average-

30 percentage method for the deseasonalization. We calculate the climatological index (over the considered period), which gives the percentage contribution of each month to the annual value. This monthly index is then applied to the timeseries to remove the seasonal component from the series. We apply the Theil-Sen estimator to estimate the linear trend magnitude

from the deseasonalized timeseries and the nonparametric Mann-Kendall test to determine the significance of the trends (95% confidence range), following the recommendation of the TOAR (Lefohn et al., 2018). We also calculate the anomalies against the mean over the entire period.

3.2 Variability and trends derived from IASI-A: 2008-2016

5   Figure 2a shows the monthly timeseries of the LT ozone column from January 2008 to December 2016 over the NCP. A large seasonal cycle with an average altitude of about 5.7 DU is observed with a maximum observed mainly in June and a minimum observed in December/January as already reported (e.g. Ding et al., 2008; Dufour et al., 2010; Hayashida et al., 2015; Safieddine et al., 2016). The interannual variability is small, about 0.15 DU (< 1%), in the first five years. A drop of 0.74 DU is observed in 2013, followed by successive decreases in 2015 and 2016 (Fig. 2b). These decreases are also seen in

10   the anomalies. The anomaly is negative during the first half of the year in 2013 and 2014 and all over the years 2015 and 2016 (Fig. 2c). Seasonal analyses of the timeseries suggest that the ozone drop observed in 2013 is mainly driven by the decrease of 1.5 DU observed in spring (MAM – March, April, May) the same year (Fig. 2d). For the other seasons, the behaviors are different but also contribute partly to the interannual variations and the significant decrease observed since 2013. LT ozone does not exhibit significant variations during the SON (September-October-November) period, except in

15   2015, where a larger decrease is observed, likely contributing to the decrease of ozone observed at the end of the period in the annual and monthly timeseries. The winter period (DJF – December, January and February) is marked by a decrease of about 2 DU between 2008 and 2013, followed by a slight increase the following years. During the summer period (JJA – June, July, August), the LT ozone increases from 2008 to 2011 (+1.2 DU) and starts a continuous decrease (except in 2014) of about -1.8 DU from 2011 to 2016. Finally, we calculate the trends from the deseasonnalized timeseries (Fig. 2e). For the

20   entire period, the trend is negative (-0.17±0.02 DU/yr, -0.774±0.001 %/yr) and significant (Mann-Kendall test). We also calculate the trend over the two distinct periods: 2008-2012 and 2013-2016. No significant trend (with slope close to zero, -0.02±0.05 DU/yr) is obtained for the first period and a significant negative trend of -0.24±0.06 DU/yr (-1.161±0.003 %/yr) is obtained for the second one. As already mentioned, similar negative trends have been reported from IASI tropospheric ozone columns in the Northern Hemisphere (Wespes et al., 2016, 2017a) with some inconsistencies with other satellite

25   observations and in situ measurements (Gaudel et al., 2018). In the following, we explore the reasons that could explain the ozone decrease observed in the LT from IASI in the NCP region impacted by the strong emission regulation during the last years (van der A et al., 2017; Li et al., 2017).

3.3 Regression model and explicative variables

Multivariate linear regression methods have been extensively used to determine the processes driving the variability and
30   trends of stratospheric (e.g. Oman et al., 2010a, 2010b; Stolarski et al., 2006) and tropospheric (e.g. Ebojie et al., 2015; Wespes et al., 2016, 2017a) ozone. Several recent studies show that several dynamical processes such as the QBO (Quasi-Biennale Oscillation), ENSO (El Nino Southern Oscillation), STE (Stratospheric-Tropospheric Exchange),... influence the

Atmospheric
Chemistry
and Physics
Discussions

variability and trends of the tropospheric ozone column (e.g. Ebojie et al., 2015; Heue et al., 2016; Oman et al., 2013; Wespes et al., 2016, 2017a, 2017b). Our study is focused on lower tropospheric ozone (below 6 km) and on a region, the NCP, where reductions of NO_x emissions have been applied in the recent years. We then expect to be more sensitive to regional emissions. In order to determine the role of dynamical and chemical processes in the ozone variability and trend

5   observed in the lower troposphere, we apply a multivariate linear regression on the deseasonalized monthly timeseries discussed previously, following Eq. (1).

$$O_3(imonth) = b + t.imonth + \sum_j m_j X_j(imonth) + \varepsilon(imonth) \qquad (1)$$

where O_3 is the deseasonalized monthly mean LT ozone, *imonth* is the month index (starting in January 2008), *b* is the intercept, *t* is the slope from which the trend is calculated, and ε is the error term. The X_j are the different normalized

10   explicative variables over the 2008-2016 period, considered in the fit, with m_j the fitting coefficients. The significance of including or not a variable is evaluated using the p-value. We consider a range of 95% confidence for the different variable tested (i.e. $p<0.05$). Each variable was tested individually first and combined then with other significant variables. The variables becoming not significant when combined with others were removed in the final fit. We have tested different dynamical variables similar to (Wespes et al., 2017b) in the regression model, related to the solar activity, the dynamical

15   processes leading to a modulation of the stratospheric circulation and of the stratospheric-tropospheric exchanges (STE) and influencing the tropospheric ozone such as the quasi-biennale oscillation (QBO), the El Nino/Southern Oscillation (ENSO). The tested variables are:

- the 10.7 cm solar radio flux. The monthly means have been calculated from the daily data, taken from the NOAA National Weather Service Climate Prediction center: ftp://ftp.ngdc.noaa.gov/STP/space-weather/solar-data/solar-
20   features/solar-radio/noontime-flux/penticton/penticton_adjusted/listings/listing_drao_noontime-flux-adjusted_daily.txt (February 2018).
- The QBO at 10 and 30 hPa are considered and summed up. They are taken from http://www.geo.fu-berlin.de/met/ag/strat/produkte/qbo/singapore.dat (February 2018).
- The Multivariate ENSO index (MEI), taken from https://www.esrl.noaa.gov/psd/enso/mei/table.html (February
25   2018).
- The tropopause height, given by the geopotential height for 2 PVU and the potential vorticity at 300 hPa. The data are taken from the ERA-interim reanalysis at http://apps.ecmwf.int/datasets/data/interim-full-daily/ (February 2018).

In addition to these dynamical variables, some chemistry-related variables used as proxies for emission changes in the NCP

30   have been also tested. In particular, we use the tropospheric NO_2 columns derived from OMI (Boersma et al., 2007, available from TEMIS database www.temis.nl) and the total CO columns derived from IASI (George et al., 2009, available from AERIS database www.aeris-data.fr). Monthly averages are calculated for the NCP domain considered in this study.

After the fitting procedure, the variables, which remain significant, are: the QBO, the potential vorticity at 300 hPa, the ENSO index, the CO total columns deseasonalized timeseries derived from IASI, and the linear trend. Their normalized

Atmospheric
Chemistry
and Physics
Discussions

timeseries are displayed in Figure 3. In order to visualize the role of each variable to explain the variability and trend of LT ozone, we plotted in Figure 4 the evolution of the residual (LT series – fit) when including the different explanatory variables as well as the deseasonalized series of the LT ozone column and the final fit. The QBO is relevant in order to account for the low frequency variations (well visible when 12-month running average is considered – not shown) and with a

5   high significance ($p<10^{-3}$), but it does not explain the decrease of LT ozone (Fig. 4 –residual QBO).

The potential vorticity (PV) at 300 hPa has been chosen in order to account for the impact of stratospheric/tropospheric exchanges on the LT ozone. Even if a significant decrease and trend are observed in the PV timeseries for the 2008-2016 period, it allows one to explain only partly the decreasing trend observed with IASI in the LT ozone. The PV variable contributes in the regression model to fit mostly winter high frequency temporal variations. As shown in Fig. 4, accounting

10 for the PV in the fit allows one to reduce the residual in February 2008 for instance, period for which strong stratospheric intrusions were already referenced in the Beijing region using IASI ozone observations (Dufour et al., 2010). Improvement in the fit residual is also observed during winters/early springs 2013 and 2014, as well as during late winter/early spring 2016. These characteristics have been found in the vertical distribution of ozone over Beijing based on ozonesondes measurements (Liu et al., 2016).

15 The next tested variable is the ENSO. Accounting for the monthly variations of the ENSO index in the regression model allows a noticeable reduction of the residual at the end of the period in 2015 and the first half of 2016. A significant part of the decrease of LT ozone is then explained by the ENSO for these last two years.

The last significant variable, we found, is the monthly CO. The timeseries of the monthly total CO column (observed by IASI) show four positive anomalies – winter 2008, winter/spring 2010, July 2012, and fall 2015 – and one major negative

20 anomaly from the beginning of 2013 to mid-2014. The positive anomalies in 2008 and 2010 allows one to significantly reduce the fitting residual and then to explain, at least partly, positive anomalies observed in the LT ozone series for the same period. The reduction of the residual for the 2015 CO anomalies is more moderate, but still present. On the contrary, the fitting residual is degraded in 2013 during the negative CO anomaly but improved in 2014.

Despite including the different explanatory variables, discussed above, including a linear trend in the regression model is still

25 necessary to improve the fitting residual. The fitted linear trend decreases from -0.17±0.02 DU/yr (linear trend only) to -0.10±0.03 DU/yr when including all these variables in the fit. Table 1 shows the evolution of the linear trend when the explanatory variables are included one by one in the fit. The main contributors are the PV at 300 hPa and the (total column) CO. This points toward two possible concomitant explanations of the trend: the first one related to a reduction of the stratospheric/tropospheric exchanges marked by the PV decrease (Fig. 3), the second one related to changes in emissions

30 whose CO might be considered as a proxy. Due to the lifetime of both CO and ozone, regional and remote sources may influence the trend over NCP, especially the global reduction of ozone precursor emission in the Northern Hemisphere. Thus, the regression model has been tested with both CO timeseries averaged for the Northern Hemisphere and CO timeseries averaged only over the NCP as explanatory variables. However, only the NCP timeseries is a significant explanatory variable in terms of p-statistics. This would suggest that changes in regional emissions would more influence the

LT ozone trend. Nevertheless, it is worth keeping in mind that the regression model represents, by nature, only the linear relationships between the variables and cannot account for the nonlinear chemistry occurring during the ozone production. One explanation of the larger significance of the NCP CO timeseries in the fit is then likely related to the similar variability of ozone and CO for some specific periods, which may be associated to emissions variability. To properly evaluate the

5 influence of regional and hemispheric emissions and their advection on the NCP LT ozone trends, use of chemistry-transport models is certainly needed but with the difficulty of having up-to-date emission inventories over the entire hemisphere for the considered time period.

4 Discussion on the reliability of the IASI derived trends

4.1 Retrieval stability

10 In this section, we evaluate the different factors that could impact the stability of the retrieval during the 2008-2016 period over the NCP. We consider the atmospheric conditions that could influence the retrieval and analyze the timerseries of related parameters. The thermal infrared measurements such as those from IASI are very sensitive to the thermal conditions of the measured scene. The surface temperature and the thermal contrast are two parameters that drive the sensitivity of the thermal infrared measurements. They can be derived from the IASI observations themselves. However, in order to be

15 independent of the IASI observations and of a possible change in the instrumental stability, we consider the skin temperature and the temperature at 2 meters from the ECMWF reanalysis (ERAinterim) to evaluate the variability and trend of these parameters over the NCP and during the 2008-2016 period. The trends are not significant with p-values of 0.08 and 0.32 for the skin temperature and the thermal contrast (calculated from the skin temperature and the 2-meter temperature), respectively. However, the skin temperature monthly timeseries show a singular change starting at the end of 2013 with

20 temperature larger especially during wintertime (Fig. 5). The thermal contrast timeseries do not reveal such a change (not shown).

The other parameter, which may influence the retrieval, is the tropopause height and its possible evolution during the considered period. Indeed, as mentioned in section 2, different constraints and a priori profiles are used, for the retrieval, depending the tropopause height. Trends in the tropopause height may then influence the retrieval. Moreover, depending on

25 the depth of the troposphere, the LT ozone column calculated up to a fixed altitude (6 km) is more or less influenced by upper tropospheric and lower stratospheric air. We consider both the tropopause height derived from the IASI temperature profiles (lapse rate method) and the tropopause given by the 2 PVU geopotential given by the ERAinterim reanalysis to evaluate the evolution of the tropopause height during the 2008-2016 period. Both datasets lead to similar monthly timeseries with a calculated trend of 0.02 km/yr, not significant (p=0.32 and p=0.15 respectively).

30 Another atmospheric condition that may influence the ozone retrievals of IASI is the presence of (coarse) aerosols. Indeed, aerosols have broad spectral signature in the spectral region used for the ozone retrieval. China is known for experiencing large aerosol loading that may affect ozone retrieval. Usually, we assume that the retrieval quality filters allow one to reject

the most affected situations. However, in order to evaluate the potential impact of aerosol loading on the retrieval and then on the derived trend, we filter out the IASI observations when the aerosol optical depth (AOD) measured by MODIS ((Hsu et al., 2013; Levy et al., 2013), https://giovanni.gsfc.nasa.gov) are larger than 0.2. Figure 5 shows the monthly timseries and the derived linear trends. Similar behavior of the ozone evolution is visible also in this subset of data with this typical change

5   in 2013. The calculated linear trend on the deseasonalized timeseries is negative (-0.19±0.04 DU/yr), similar to the trend derived for the entire set of data, and significant (p < 10^{-3}).

Finally, we based our evaluation of the retrieval stability to the analysis of the averaging kernels (AK). Indeed, they integrate and translate the retrieval sensitivity to the atmospheric conditions (temperature, pressure, etc changes). We consider two related variables: the degrees of freedom (DOF) of the retrieval, calculated as the sum of the diagonal elements of the AK

10   matrix, and the altitude of the maximum sensitivity of the retrieval. The DOF and the altitude of maximum sensitivity are calculated for the LT ozone column. The resulting monthly timeseries averaged over the NCP are displayed in Fig. 5. The linear trends derived for these two variables are increasing (0.002 per year) for the DOF and decreasing (-0.02 km/yr) for the altitude of maximum sensitivity but with a slight significance (p=0.06 and p=0.12 respectively). The temporal evolution of these two parameters would suggest the retrieval sensitivity of the LT ozone increases over time. This would points toward a

15   slightly lesser contamination of the LT retrieved columns from higher altitudes where ozone is usually larger, and then possibly smaller LT columns. However, the changes are very small and only slightly statistically significant to draw clear conclusions at this stage. Finally another way to evaluate the retrieval stability based on the AK is to consider one unique ozone profile and the associated pressure and temperature profiles taken from a chemistry-transport model – here the LMDz-INCA model (Hauglustaine et al., 2004) – and to apply the averaging kernels of each individual IASI pixel retrieved for the

20   entire 2008-2016 period to this profile. The variations observed on the resulting profiles translates the possible changes in terms of retrieval sensitivity as well as the changes in the meteorology, surface conditions, etc., that can influence the retrieval sensitivity (and then the averaging kernels). The resulting monthly timeseries are displayed in Fig. 6. The linear trend calculated from the deseasonalized timerseries is negligeable (0.005 DU/yr) and not significant (p=0.79). Thus, these results suggest that no significant trend can be attributed to a change in the retrieval sensitivity for the NCP, the considered

25   region in this study, during the 2008-2016 period.

4.2 Comparison with the independent IASI-B ozone observations

The results presented in the previous sections are obtained from the IASI instrument flying on the Metop-A satellite. Since February 2013, the second IASI instrument aboard the Metop-B satellite has been providing data. In this section, we use the IASI-B instrument for the period 2013-2016 and compare the monthly timeseries and trends to those derived from the IASI-

30   A instrument. For the comparison of the two instruments, the monthly averages are calculated from daily (morning overpass) gridded data at a resolution of 0.25°. The grid cells considered in the average are those for which data are available for the two instruments. Figure 7 shows the results of the comparison. A positive bias of +0.41 DU (+2%) is observed on average between IASI-B and IASI-A. This is in agreement with the results reported by Boynard et al. (2016, 2018) for tropospheric

ozone, obtained with a different retrieval algorithm. The trends derived from IASI-A and IASI-B from deseasonalized timeseries (Fig. 7) are very similar, -0.33±0.05 DU/yr and -0.32±0.06 DU/yr, respectively. For comparison, the trend derived for the same period with all the IASI-A data considered, not only those in coincidence with IASI-B, is -0.24±0.06 DU/yr. Then, the comparison of IASI-A and IASI-B confirms that the trend derived from IASI-A for the period 2013-2016 is not to

5   be attributed to an instrumental drift or an instrumental failure of IASI-A as the IASI-B instrument provides independent measurements.

4.3 Comparison with ozonesonde measurements

We also performed a validation by comparing the IASI observations with ozonesonde measurements available in the East
10   Asian region. We use the same method for the comparison than those described in Dufour et al. (2012, 2015). We compare IASI ozone columns to the ozonesonde columns smoothed with the IASI averaging kernels. Five ozonesonde stations are used for the validation. They are listed, as well as the obtained results, in Table 2. The covered time period extends from 2008 to 2015 (at the time of the study, the sonde data were not available for the entire year 2016 for all the sondes). The coincidence criteria used for the present validation exercise are 1° around the station, a time difference smaller than 12h, and
15   a minimum of 10 cloud-free pixels matching the two previous criteria. The criterion on the time difference has been released compared to a previous study (Dufour et al., 2015) in order to have a more statistically-significant number of coincidences for all the stations.

The bias between IASI observations and ozonesondes measurements is negative and ranges from -3% (Sapporo) to -26% (Beijing). It is worth noting that the instrumentation of the Beijing ozonesonde has changed in 2013. Comparisons with IASI
20   before 2013 show a negative bias of about -26%, whereas the bias decreases to -11% in 2014, being in better agreement with other Asian sondes (Zhang et al., 2014). On average, the bias for the Asian stations is about -10 to -15%, IASI underestimating the LT ozone columns. We also compare the results for the first four years of the period and the last four years of the period (Table 2). We observe a degradation of the comparison results between IASI and the sonde at the beginning and the end of the period. For example, the negative bias increases from 10% to 14% at the Tateno station and the
25   correlation coefficient decreases from 0.87 to 0.75. The number of days with coincident measurements is not that high (about 20 to 25 per year per sonde) for the Asian stations. It may introduce a sampling issue, which could explain this difference. To prove this, we choose the midlatitude European station with the largest number of available measurements, the Payerne station to do another comparison. In that case, a small bias of +2.8% is observed but with a poor correlation (Table 2). We also observed a significant change in the bias from the beginning to the end of the period. Looking at the results in details, it
30   arises that the winter period was not sampled (no coincidence) for three years over four during the beginning of the period (2008-2011). Filtering out the winter period (DJF) in the comparison IASI/sonde leads to a much better agreement with a tiny bias (-0.12%) and a good correlation (r=0.68), and no significant degradation of the comparison between the beginning and the end of the period (Table 2, last row). However, removing winter season in the comparison for the Asian sondes does

not improve the comparison, except slightly for Sapporo. We also compared IASI-B and IASI-A LT ozone columns to the ozonesonde measurements for the 2013-2016 period, using only days for which observations are available for the three datasets. We obtain very similar results. For example, the bias for the Tateno sondings is the same (-15%) and the correlation coefficient is slightly improved with IASI-B (0.71 against 0.65).

5 Despite the poor temporal sampling frequency of the ozonesondes (at the best about four per month for Asian sondes), we calculate the slope of the seasonal timeseries for the IASI and smoothed ozonesonde LT columns for each station, as a first approximation of the trend (Table 2). Almost none of the slope is statistically significant. This is clearly visible with the standard deviations larger than the slopes themselves. The only soundings for which the slope is (slightly) significant are the Payerne station with a good agreement when winter measurements are not considered (see discussion above), the Tateno and

10 the Sapporo stations with a poor agreement. Figure 8 compares the annual variations of IASI LT columns and sondes LT columns, both without and with averaging kernels applied for the four Asian ozonesondes. Whereas IASI exhibits rather small interannual variability and relatively flat timeseries, the ozonesondes, especially in the Tateno and Sapporo stations, exhibit an increase in 2010-2011 with stabilization the following years. This is clearly visible on the raw sounding (i.e. without averaging kernel smoothing). One possible explanation for this increase is the change of the used technology for the

15 sondes. The sounding technology has moved from KC-96 sondes to ECC sondes in December 2009 for Tateno and Sapporo soundings (Morris et al., 2013). This increase translates into the slopes we can calculate from ozonesondes leading to positive slopes (Table 2). In order to test the sensitivity of the derived slope, especially its sign, to the number of samples, we use the Tateno station during the IASI-B period during which no instrumental change was made on the sondes. We calculate the slope for the Tateno ozonesondes in two situations: (i) when IASI-A, IASI-B, and the sondes match the coincindence

20 criteria (30 days sampled), (ii) when IASI-B only and the sondes match the concidence criteria (48 days sampled). The slopes we obtain are: -0.03±0.2 (DU) and 0.26 ±0.2 (DU), respectively for the sonde measurements and -0.31±0.2 (DU) and 0.15±0.2 (DU), respectively for IASI-B. As expected in the case of poor sampling as for the sondes, changing the number of samples can change completely the slope of the linear regression and change the sign of the slopes in this particular case. This combined with the instrumentation changes for some stations (Beijing, Tateno, Sapporo) stresses the limitation of using

25 ozonesondes to evaluate the trends derived from satellite observations in our case.

4.4 Comparison with in situ surface measurements

We compare the IASI LT columns, converted into equivalent volume mixing ratios, to surface measurements made at the Shangdianzi station, China. The Shangdianzi station is a regional Global Atmosphere Watch (GAW) station, located about

30 100 km northeast of Beijing and classified as a rural station. Previous studies suggest that the pollutant observations at this station are representative of the regional-scale air quality of the NCP (Lin et al., 2008; Xu et al., 2009). IASI observations within 0.25°x0.25° around the stations are considered (40.5°N-40.75°, 117°E-117.25°E). Obviously, the quantities are not completely comparable as we compare columns and surface measurements and as IASI is poorly sensitive to the surface

(Cuesta et al., 2017) but the focus here is to evaluate the sampling effect. When considering all the surface data (every day, every hour), the linear trend calculated from the deseasonalized timeseries for the surface station (Fig. 9, first row) is positive (slightly significant, p=0.09), whereas the IASI trend (calculated only for clear-sky days) is significantly negative. Then, we consider only daytime (8-20h local time) surface observations, which should be more representative of IASI observations.

5 Indeed, IASI observations are made during the day and more representative of the free troposphere or of highly developed planetary boundary layers (PBL) (Eremenko et al., 2008) and cannot be compared to nighttime observations when the PBL is isolated from the free troposphere. The calculated linear trend of the daytime surface measurement is still positive, but reduces and becomes poorly significant (Fig. 9, 2nd row). Then, we consider daytime surface observations only the days for which IASI data are available. The calculated linear trend becomes negative (not significant, Fig. 9, 3rd row). We also test to

10 consider the surface measurement the day after the IASI data are available. Indeed, a recent study shows the downward mixing of free tropospheric ozone may largely impact the morning level of ozone in the surface layer, the surface ozone level on one day being likely related with ozone at higher levels the day before (Wang et al., 2017a). In that case, the calculated trend is even more negative but still poorly significant (Fig. 9, 4th row). These results show the sensitivity of the trend calculation to the sampling (day/night, clear-sky conditions) and stress the need to compare datasets with different

15 temporal sampling frequency over subsets of data with consistent sampling before drawing conclusions, especially in terms of trend comparison.

5 Conclusions

The analysis of the LT ozone columns retrieved from the IASI-A instrument over the NCP between 2008 and 2016 shows a negative trend of ozone in the lower troposphere with 2013 being a pivotal year. Before 2013, no trend is detected whereas a

20 significant negative trend of -0.24±0.06 DU/yr (-1.161±0.003 %/yr) is derived for 2013-2016. A similar trend is observed with the second IASI instrument in flight, IASI-B, for the same period. We explore the dynamical and chemical factors that could explain this overall negative trend using a multivariate regression model. The results suggest that the negative trend observed from IASI could arise from a reduction of the stratosphere-to-troposphere transport combined with reduction of regional precursor emissions, as suggested by the PV at 300 hPa and the used CO proxy, respectively. Due to previous

25 studies, especially based on surface measurements (e.g. Ma et al., 2016), showing an increase of ozone at the surface in the NCP, our results presenting negative trends were surprising. We then also explore the possibility of instabilities in the retrieval that could explain the observed negative trend with IASI. The analysis of internal and external parameters that could affect the retrieval does not show any evidence of instrumental instability or drift over the NCP for the considered period. Moreover, comparison with the independent IASI-B instrument shows similar decrease of ozone after 2013. A recent

30 work comparing tropospheric ozone trends derived from IR and UV satellite sounders reveal an inconsistency between these two kinds of observations (Gaudel et al., 2018), with IR sounders showing a general negative trend (Oetjen et al., 2015; Wespes et al., 2017a) and UV sounders a general positive trend (Cooper et al., 2014). One hypothesis made to explain this

Atmospheric
Chemistry
and Physics
Discussions

Open Access

EGU

discrepancy lies on the difference in the vertical sensitivity of the IR and UV instruments but without clear evidence of this issue found. One key point, which has been revealed by the comparisons made in the present study, concerns the impact of the sampling on the derived trends. This questions about how representative are the trends derived from the different datasets and stresses the need of intercomparisons made on sub datasets presenting similar sampling.

5   Finally, although the LT ozone column and surface ozone level are different quantities, it is not straightforward why the LT ozone showed a negative trend while the surface ozone a positive one (e.g. Ma et al., 2016). If both trends are reliable, a possible explanation to this inconsistency may be that the LT and surface ozone responded differently to the recent reduction of NO_x. Previous ozone production efficiency studies (Ge et al., 2010, 2012) suggest that even at the background site of the NCP, ozone production in the surface layer seemed to be more VOC-limited. Although Chinese NO_x emissions have been

10   reduced in recent years, that VOCs emissions have been continuously increasing (Li et al., 2017). The observed recent decline of tropospheric NO_2 (van der A et al., 2017) might have contributed mainly to the decrease of ozone at the levels above the surface layer, where ozone production is more sensitive to NO_x. To better understand the changes of ozone at different altitudes over the NCP, more observations from different platforms as well as modeling studies are necessary.

Acknowledgements

References

van der A, R. J., Mijling, B., Ding, J., Koukouli, M. E., Liu, F., Li, Q., Mao, H. and Theys, N.: Cleaning up the air: effectiveness of air quality policy for SO2 and NOx emissions in China, Atmos. Chem. Phys., 17(3), 1775–1789,
30   doi:10.5194/acp-17-1775-2017, 2017.

Boersma, K. F., Eskes, H. J., Veefkind, J. P., Brinksma, E. J., van der A, R. J., Sneep, M., van den Oord, G. H. J., Levelt, P. F., Stammes, P., Gleason, J. F. and Bucsela, E. J.: Near-real time retrieval of tropospheric NO2from OMI, Atmos. Chem. Phys., 7(8), 2103–2118, doi:10.5194/acp-7-2103-2007, 2007.

Boynard, A., Hurtmans, D., Koukouli, M. E., Goutail, F., Bureau, J., Safieddine, S., Lerot, C., Hadji-Lazaro, J., Wespes, C.,

13

Pommereau, J.-P., Pazmino, A., Zyrichidou, I., Balis, D., Barbe, A., Mikhailenko, S. N., Loyola, D., Valks, P., Van Roozendael, M., Coheur, P.-F. and Clerbaux, C.: Seven years of IASI ozone retrievals from FORLI: validation with independent total column and vertical profile measurements, Atmos. Meas. Tech., 9(9), 4327–4353, doi:10.5194/amt-9-4327-2016, 2016.

5   Boynard, A., Hurtmans, D., Garane, K., Goutail, F., Hadji-Lazaro, J., Koukouli, M. E., Wespes, C., Keppens, A., Pommereau, J.-P., Pazmino, A., Balis, D., Loyola, D., Valks, P., Coheur, P.-F. and Clerbaux, C.: Validation of the IASI FORLI/Eumetsat ozone products using satellite (GOME-2), ground-based (Brewer-Dobson, SAOZ) and ozonesonde measurements, Atmos. Meas. Tech. Discuss., 1–35, doi:10.5194/amt-2017-461, 2018.

Chen, X., Huang, F. X., Xia, X. Q., Cao, J. and Xu, X.: Analysis of tropospheric ozone long-term changing trends and
10   affecting factors over northern China (in Chinese), Chin Sci Bull, 60, 2659–2666, doi:10.1360/N972015–00155, 2015.

Clerbaux, C., Boynard, A., Clarisse, L., George, M., Hadji-Lazaro, J., Herbin, H., Hurtmans, D., Pommier, M., Razavi, A., Turquety, S., Wespes, C. and Coheur, P.-F.: Monitoring of atmospheric composition using the thermal infrared IASI/MetOp sounder, Atmos. Chem. Phys., 9(16), 6041–6054, doi:10.5194/acp-9-6041-2009, 2009.

Cooper, O. R., Parrish, D. D., Ziemke, J., Balashov, N. V., Cupeiro, M., Galbally, I. E., Gilge, S., Horowitz, L., Jensen, N.
15   R., Lamarque, J.-F., Naik, V., Oltmans, S. J., Schwab, J., Shindell, D. T., Thompson, A. M., Thouret, V., Wang, Y. and Zbinden, R. M.: Global distribution and trends of tropospheric ozone: An observation-based review, Elem. Sci. Anthr., 2(1), 29, doi:10.12952/journal.elementa.000029, 2014.

Cuesta, J., Kanaya, Y., Takigawa, M., Dufour, G., Eremenko, M., Foret, G., Miyazaki, K. and Beekmann, M.: Transboundary ozone pollution across East Asia: daily evolution and photochemical production analysed by IASI+GOME2
20   multispectral satellite observations and models, Atmos. Chem. Phys. Discuss., 1–51, doi:10.5194/acp-2017-972, 2017.

Van Damme, M., Whitburn, S., Clarisse, L., Clerbaux, C., Hurtmans, D. and Coheur, P.-F.: Version 2 of the IASI NH&lt;sub&gt;3&lt;/sub&gt; neural network retrieval algorithm: near-real-time and reanalysed datasets, Atmos. Meas. Tech., 10(12), 4905–4914, doi:10.5194/amt-10-4905-2017, 2017.

Ding, A. J., Wang, T., Thouret, V., Cammas, J.-P. and Nédélec, P.: Tropospheric ozone climatology over Beijing: analysis of
25   aircraft data from the MOZAIC program, Atmos. Chem. Phys., 8(1), 1–13, doi:10.5194/acp-8-1-2008, 2008.

Dufour, G., Eremenko, M., Orphal, J. and Flaud, J.-M.: IASI observations of seasonal and day-to-day variations of tropospheric ozone over three highly populated areas of China: Beijing, Shanghai, and Hong Kong, Atmos. Chem. Phys., 10(8), 3787–3801, doi:10.5194/acp-10-3787-2010, 2010.

Dufour, G., Eremenko, M., Griesfeller, a., Barret, B., Leflochmoën, E., Clerbaux, C., Hadji-Lazaro, J., Coheur, P. F. and
30   Hurtmans, D.: Validation of three different scientific ozone products retrieved from IASI spectra using ozonesondes, Atmos. Meas. Tech., 5(3), 611–630, doi:10.5194/amt-5-611-2012, 2012.

Dufour, G., Eremenko, M., Cuesta, J., Doche, C., Foret, G., Beekmann, M., Cheiney, A., Wang, Y., Cai, Z., Liu, Y., Takigawa, M., Kanaya, Y. and Flaud, J.-M.: Springtime daily variations in lower-tropospheric ozone over east Asia: the role of cyclonic activity and pollution as observed from space with IASI, Atmos. Chem. Phys., 15(18), 10839–10856,

doi:10.5194/acp-15-10839-2015, 2015.

Ebojie, F., Burrows, J. P., Gebhardt, C., von Savigny, C., Rozanov, A., Weber, M. and Bovensmann, H.: Global and zonal tropospheric ozone variations from 2003–2011 as seen by SCIAMACHY, Atmos. Chem. Phys. Discuss., 15(17), 24085–24130, doi:10.5194/acpd-15-24085-2015, 2015.

5 Ebojie, F., Burrows, J. P., Gebhardt, C., Ladstätter-Weißenmayer, A., von Savigny, C., Rozanov, A., Weber, M. and Bovensmann, H.: Global tropospheric ozone variations from 2003 to 2011 as seen by SCIAMACHY, Atmos. Chem. Phys., 16(2), 417–436, doi:10.5194/acp-16-417-2016, 2016.

Eremenko, M., Dufour, G., Foret, G., Keim, C., Orphal, J., Beekmann, M., Bergametti, G. and Flaud, J. M.: Tropospheric ozone distributions over Europe during the heat wave in July 2007 observed from infrared nadir spectra recorded by IASI,

10 Geophys. Res. Lett., 35(18), 0–4, doi:10.1029/2008GL034803, 2008.

Gaudel, A., Cooper, O. R., Ancellet, G., Barret, B., Boynard, A., Burrows, J. P., Clerbaux, C., Coheur, P.-F., Cuesta, J., Cuevas, E., Doniki, S., Dufour, G., Ebojie, F., Foret, G., Garcia, O., Munos, M. J. G., Hannigan, J. W., Hase, F., Huang, G., Hassler, B., Hurtmans, D., Jaffe, D. A., Jones, N., Kalabokas, P., Kerridge, B., Kulawik, S., Latter, B., Leblanc, T., Le Flochmoën, E., Lin, W., Liu, J., Liu, X., Mahieu, E., McClure-Begley, A., Neu, J., Osman, M., Palm, M., Petetin, H.,

15 Petropavlovskikh, I., Querel, R., Rahpoe, N., Rozanov, A., Schultz, M. G., Schwab, J., Siddans, R., Smale, D., Steinbacher, M., Tanimoto, H., Tarasick, D. W., Thouret, V., Thompson, A. M., Trickl, T., Weatherhead, E., Wespes, C., Worden, H. M., Vigouroux, C., Xu, X., Zeng, G. and Ziemke, J. R.: Tropospheric Ozone Assessment Report : Present-day distribution and trends of tropospheric ozone relevant to climate and global atmospheric chemistry model evaluation, Elem. Sci. Anthr., in revision, 2018.

20 Ge, B., Xu, X., Lin, W. and Wang, Y.: Observational Study of Ozone Production Efficiency at the Shangdianzi Regional Background Station, Chinese J. Environ. Sci., 31(7), 1444–1450 [online] Available from: https://caod.oriprobe.com/articles/25273572/Observational_Study_of_Ozone_Production_Efficiency.htm (Accessed 23 April 2018), 2010.

Ge, B. Z., Xu, X. B., Lin, W. L., Li, J. and Wang, Z. F.: Impact of the regional transport of urban Beijing pollutants on

25 downwind areas in summer: ozone production efficiency analysis, Tellus B Chem. Phys. Meteorol., 64(1), 17348, doi:10.3402/tellusb.v64i0.17348, 2012.

George, M., Clerbaux, C., Hurtmans, D., Turquety, S., Coheur, P.-F., Pommier, M., Hadji-Lazaro, J., Edwards, D. P., Worden, H., Luo, M., Rinsland, C. and McMillan, W.: Carbon monoxide distributions from the IASI/METOP mission: evaluation with other space-borne remote sensors, Atmos. Chem. Phys., 9(21), 8317–8330, doi:10.5194/acp-9-8317-2009,

30 2009.

Hauglustaine, D. A., Hourdin, F., Jourdain, L., Filiberti, M.-A., Walters, S., Lamarque, J.-F. and Holland, E. A.: Interactive chemistry in the Laboratoire de Météorologie Dynamique general circulation model: Description and background tropospheric chemistry evaluation, J. Geophys. Res., 109(D4), D04314, doi:10.1029/2003JD003957, 2004.

Hayashida, S., Liu, X., Ono, A., Yang, K. and Chance, K.: Observation of ozone enhancement in the lower troposphere over

East Asia from a space-borne ultraviolet spectrometer, Atmos. Chem. Phys. Discuss., 15(2), 2013–2054, doi:10.5194/acpd-15-2013-2015, 2015.

Heue, K.-P., Coldewey-Egbers, M., Delcloo, A., Lerot, C., Loyola, D., Valks, P. and van Roozendael, M.: Trends of tropical tropospheric ozone from 20 years of European satellite measurements and perspectives for the Sentinel-5 Precursor, Atmos.

5 Meas. Tech., 9(10), 5037–5051, doi:10.5194/amt-9-5037-2016, 2016.

Hsu, N. C., Jeong, M.-J., Bettenhausen, C., Sayer, A. M., Hansell, R., Seftor, C. S., Huang, J. and Tsay, S.-C.: Enhanced Deep Blue aerosol retrieval algorithm: The second generation, J. Geophys. Res. Atmos., 118(16), 9296–9315, doi:10.1002/jgrd.50712, 2013.

Kulawik, S. S., Osterman, G., Jones, D. B. A. and Bowman, K. W.: Calculation of altitude-dependent tikhonov constraints

10 for TES nadir retrievals, IEEE Trans. Geosci. Remote Sens., 44(5), 1334–1342, doi:10.1109/TGRS.2006.871206, 2006.

Lefohn, A. S., Malley, C. S., Smith, L., Wells, B., Hazucha, M., Simon, H., Naik, V., Mills, G., Schultz, M. G., Paoletti, E., De Marco, A., Xu, X., Zhang, L., Wang, T., Neufeld, H. S., Musselman, R. C., Tarasick, D., Brauer, M., Feng, Z., Tang, H., Kobayashi, K., Sicard, P., Solberg, S. and Gerosa, G.: Tropospheric ozone assessment report: Global ozone metrics for climate change, human health, and crop/ecosystem research, Elem Sci Anth, 6(1), 28, doi:10.1525/elementa.279, 2018.

15 Levy, R. C., Mattoo, S., Munchak, L. A., Remer, L. A., Sayer, A. M., Patadia, F. and Hsu, N. C.: The Collection 6 MODIS aerosol products over land and ocean, Atmos. Meas. Tech., 6(11), 2989–3034, doi:10.5194/amt-6-2989-2013, 2013.

Li, M., Liu, H., Geng, G., Hong, C., Liu, F., Song, Y., Tong, D., Zheng, B., Cui, H., Man, H., Zhang, Q. and He, K.: Anthropogenic emission inventories in China: a review, Natl. Sci. Rev., 4(6), 834–866, doi:10.1093/nsr/nwx150, 2017.

Lin, M., Horowitz, L. W., Cooper, O. R., Tarasick, D., Conley, S., Iraci, L. T., Johnson, B., Leblanc, T., Petropavlovskikh, I.

20 and Yates, E. L.: Revisiting the evidence of increasing springtime ozone mixing ratios in the free troposphere over western North America, Geophys. Res. Lett., 42(20), 8719–8728, doi:10.1002/2015GL065311, 2015.

Lin, M., Horowitz, L. W., Payton, R., Fiore, A. M. and Tonnesen, G.: US surface ozone trends and extremes from 1980 to 2014: quantifying the roles of rising Asian emissions, domestic controls, wildfires, and climate, Atmos. Chem. Phys., 17(4), 2943–2970, doi:10.5194/acp-17-2943-2017, 2017.

25 Lin, W., Xu, X., Zhang, X. and Tang, J.: Contributions of pollutants from North China Plain to surface ozone at the Shangdianzi GAW Station, Atmos. Chem. Phys., 8(19), 5889–5898, doi:10.5194/acp-8-5889-2008, 2008.

Liu, C. X., Liu, Y. and Wang, Y.: Vertical distribution of ozone over Beijing from GPSO3 in-situ measurements, J. Meteorol. Environ., 32(1), 46–52, 2016.

Ma, Z., Xu, J., Quan, W., Zhang, Z., Lin, W. and Xu, X.: Significant increase of surface ozone at a rural site, north of eastern

30 China, Atmos. Chem. Phys., 16(6), 3969–3977, doi:10.5194/acp-16-3969-2016, 2016.

McPeters, R. D., Labow, G. J. and Logan, J. A.: Ozone climatological profiles for satellite retrieval algorithms, J. Geophys. Res., 112(D5), D05308, doi:10.1029/2005JD006823, 2007.

Morris, G. A., Labow, G., Akimoto, H., Takigawa, M., Fujiwara, M., Hasebe, F., Hirokawa, J. and Koide, T.: On the use of the correction factor with Japanese ozonesonde data, Atmos. Chem. Phys., 13(3), 1243–1260, doi:10.5194/acp-13-1243-

2013, 2013.

Neu, J. L., Flury, T., Manney, G. L., Santee, M. L., Livesey, N. J. and Worden, J.: Tropospheric ozone variations governed by changes in stratospheric circulation, Nat. Geosci., 7(5), 340–344, doi:10.1038/ngeo2138, 2014.

Oetjen, H., Payne, V. H., Neu, J. L., Kulawik, S. S., Edwards, D. P., Eldering, A., Worden, H. M. and Worden, J. R.: A Joint

5   data record of tropospheric ozone from Aura-TES and MetOp-IASI, Atmos. Chem. Phys. Discuss., 15(21), 31025–31051, doi:10.5194/acpd-15-31025-2015, 2015.

Oman, L. D., Waugh, D. W., Kawa, S. R., Stolarski, R. S., Douglass, A. R. and Newman, P. A.: Mechanisms and feedback causing changes in upper stratospheric ozone in the 21st century, J. Geophys. Res., 115(D5), D05303, doi:10.1029/2009JD012397, 2010a.

10   Oman, L. D., Plummer, D. A., Waugh, D. W., Austin, J., Scinocca, J. F., Douglass, A. R., Salawitch, R. J., Canty, T., Akiyoshi, H., Bekki, S., Braesicke, P., Butchart, N., Chipperfield, M. P., Cugnet, D., Dhomse, S., Eyring, V., Frith, S., Hardiman, S. C., Kinnison, D. E., Lamarque, J.-F., Mancini, E., Marchand, M., Michou, M., Morgenstern, O., Nakamura, T., Nielsen, J. E., Olivié, D., Pitari, G., Pyle, J., Rozanov, E., Shepherd, T. G., Shibata, K., Stolarski, R. S., Teyssèdre, H., Tian, W., Yamashita, Y. and Ziemke, J. R.: Multimodel assessment of the factors driving stratospheric ozone evolution over the

15   21st century, J. Geophys. Res. Atmos., 115(D24), doi:10.1029/2010JD014362, 2010b.

Oman, L. D., Douglass, A. R., Ziemke, J. R., Rodriguez, J. M., Waugh, D. W. and Nielsen, J. E.: The ozone response to ENSO in Aura satellite measurements and a chemistry-climate simulation, J. Geophys. Res. Atmos., 118(2), 965–976, doi:10.1029/2012JD018546, 2013.

Richter, A., Burrows, J. P., Nüß, H., Granier, C. and Niemeier, U.: Increase in tropospheric nitrogen dioxide over China

20   observed from space, Nature, 437(7055), 129–132, doi:10.1038/nature04092, 2005.

Safieddine, S., Boynard, A., Hao, N., Huang, F., Wang, L., Ji, D., Barret, B., Ghude, S. D., Coheur, P.-F., Hurtmans, D. and Clerbaux, C.: Tropospheric ozone variability during the East Asian summer monsoon as observed by satellite (IASI), aircraft (MOZAIC) and ground stations, Atmos. Chem. Phys., 16(16), 10489–10500, doi:10.5194/acp-16-10489-2016, 2016.

Stolarski, R. S., Douglass, A. R., Steenrod, S., Pawson, S., Stolarski, R. S., Douglass, A. R., Steenrod, S. and Pawson, S.:

25   Trends in Stratospheric Ozone: Lessons Learned from a 3D Chemical Transport Model, J. Atmos. Sci., 63(3), 1028–1041, doi:10.1175/JAS3650.1, 2006.

Sun, L., Xue, L., Wang, T., Gao, J., Ding, A., Cooper, O. R., Lin, M., Xu, P., Wang, Z., Wang, X., Wen, L., Zhu, Y., Chen, T., Yang, L., Wang, Y., Chen, J. and Wang, W.: Significant increase of summertime ozone at Mount Tai in Central Eastern China, Atmos. Chem. Phys., 16(16), 10637–10650, doi:10.5194/acp-16-10637-2016, 2016.

30   Tang, G., Li, X., Wang, Y., Xin, J. and Ren, X.: Surface ozone trend details and interpretations in Beijing, 2001–2006, Atmos. Chem. Phys., 9(22), 8813–8823, doi:10.5194/acp-9-8813-2009, 2009.

Tikhonov, A.: On the Solution of Incorrectly Stated Problems and a Method of Regularisation, Dokl. Acad. Nauk SSSR, 151, 501–504, 1963.

Verstraeten, W. W., Neu, J. L., Williams, J. E., Bowman, K. W., Worden, J. R. and Boersma, K. F.: Rapid increases in

Atmospheric
Chemistry
and Physics
Discussions

tropospheric ozone production and export from China, Nat. Geosci., 8(9), 690–695, doi:10.1038/ngeo2493, 2015.

Wang, R., Xu, X., Jia, S., Ma, R., Ran, L., Deng, Z., Lin, W., Wang, Y. and Ma, Z.: Lower tropospheric distributions of O3 and aerosol over Raoyang, a rural site in the North China Plain, Atmos. Chem. Phys., 17(6), 3891–3903, doi:10.5194/acp-17-3891-2017, 2017a.

5 Wang, T., Wei, X. L., Ding, A. J., Poon, C. N., Lam, K. S., Li, Y. S., Chan, L. Y. and Anson, M.: Increasing surface ozone concentrations in the background atmosphere of Southern China, 1994–2007, Atmos. Chem. Phys., 9(16), 6217–6227, doi:10.5194/acp-9-6217-2009, 2009.

Wang, W.-N., Cheng, T.-H., Gu, X.-F., Chen, H., Guo, H., Wang, Y., Bao, F.-W., Shi, S.-Y., Xu, B.-R., Zuo, X., Meng, C. and Zhang, X.-C.: Assessing Spatial and Temporal Patterns of Observed Ground-level Ozone in China., Sci. Rep., 7(1),
10 3651, doi:10.1038/s41598-017-03929-w, 2017b.

Wang, Y., Konopka, P., Liu, Y., Chen, H., Müller, R., Plöger, F., Riese, M., Cai, Z. and Lü, D.: Tropospheric ozone trend over Beijing from 2002–2010: ozonesonde measurements and modeling analysis, Atmos. Chem. Phys., 12(18), 8389–8399, doi:10.5194/acp-12-8389-2012, 2012.

Wespes, C., Hurtmans, D., Emmons, L. K., Safieddine, S., Clerbaux, C., Edwards, D. P. and Coheur, P.-F.: Ozone variability
15 in the troposphere and the stratosphere from the first 6 years of IASI observations (2008–2013), Atmos. Chem. Phys., 16(9), 5721–5743, doi:10.5194/acp-16-5721-2016, 2016.

Wespes, C., Hurtmans, D., Clerbaux, C., Boynard, A. and Coheur, P.-F.: Decrease in tropospheric O3 levels of the Northern Hemisphere observed by IASI, Atmos. Chem. Phys. Discuss., 1–33, doi:10.5194/acp-2017-904, 2017a.

Wespes, C., Hurtmans, D., Clerbaux, C. and Coheur, P.-F.: O 3 variability in the troposphere as observed by IASI over 2008-
20 2016: Contribution of atmospheric chemistry and dynamics, J. Geophys. Res. Atmos., 122(4), 2429–2451, doi:10.1002/2016JD025875, 2017b.

WMO: International list of selected and supplementary ships, 3, WMO 47 (WMO/OMM 47, TP. 18), 143 pp.,., 1957.

Xu, W., Lin, W., Xu, X., Tang, J., Huang, J., Wu, H. and Zhang, X.: Long-term trends of surface ozone and its influencing factors at the Mt Waliguan GAW station, China – Part 1: Overall trends and characteristics, Atmos. Chem. Phys., 16(10),
25 6191–6205, doi:10.5194/acp-16-6191-2016, 2016.

Xu, W., Xu, X., Lin, M., Lin, W., Tarasick, D., Tang, J., Ma, J. and Zheng, X.: Long-term trends of surface ozone and its influencing factors at the Mt Waliguan GAW station, China – Part 2: The roles of anthropogenic emissions and climate variability, Atmos. Chem. Phys., 18(2), 773–798, doi:10.5194/acp-18-773-2018, 2018.

Xu, X. and Lin, W.: Trends of Tropospheric Ozone over China Based on Satellite Data (1979–2005), Adv. Clim. Chang.
30 Res., 2(1), 43–48, doi:10.3724/SP.J.1248.2011.00043, 2011.

Xu, X. B., Liu, X. W. and Lin, W. L.: Impacts of air parcel transport on the contrations of trace gases at regional background stations (in Chinese), J. Appl. Meteorol. Sci., 20, 656–664, 2009.

Zhang, J., Xuan, Y., Yan, X., Liu, M., Tian, H., Xia, X., Pang, L. and Zheng, X.: Development and preliminary evaluation of a double-cell ozonesonde, Adv. Atmos. Sci., 31(4), 938–947, doi:10.1007/s00376-013-3104-1, 2014.

Atmospheric
Chemistry
and Physics
Discussions

Table 1: Evolution of the fitted linear trend and the residual when explanatory variables are included one by one in the fitting procedure.

Explanatory variable	Fitted linear trend (DU/yr)	Residual standard deviation
Linear trend	-0.17±0.02	0.61
+ QBO	-0.16±0.02	0.58
+ PV @ 300hPa	-0.14±0.02	0.54
+ ENSO	-0.13±0.03	0.54
+ CO	-0.10±0.03	0.51

Table2: Statistics of the IASI and ozonesondes comparisons

Sonde[a]		2008-2015				2008-2011		2012-2015	
	ndays	Bias (DU/%)	r	Slope[c] IASI	Slope[c] sonde	Bias (DU/%)	r	Bias (DU/%)	r
Naha	186	-3.2/-14	0.77	-0.01±0.03	0.03±0.07	-2.6/-11	0.84	-3.8/-16	0.77
Hong Kong	188	-2.5/-11	0.54	0.02±0.03	0.02±0.03	-2.5/-11	0.69	-2.5/-11	0.39
Sapporo	149	-0.7/-3.2	0.07	-0.006±0.04	0.056±0.04	-0.28/-1.3	0.26	-1.2/-4.9	0.11
Tateno	174	-3.0/-12	0.81	-0.002±0.04	0.07±0.05	-2.4/-10	0.87	-3.5/-14	0.75
Beijing[b]	106	-7.9/-26	0.60	-0.075±0.06	-0.25±0.13				
Payerne	257	0.53/2.8	0.17	-0.014±0.03	-0.04±0.02	-0.01/-0.07	0.55	1.0/5.4	0.03
w/o DJF		-0.02/-0.12	0.68	-0.03±0.02	-0.03±0.02	-0.18/-0.94	0.65	0.05/0.25	0.68

[a] the correction factor is not considered to filter the data (no significant changes), except for Beijing, where only sonde measurement with a correction factor ranged between 0.8 and 1.2 are considered.

[b] data are available only for the 2008-2014 period with a gap in 2013 due to instrumentation changes.

[c] the slope is calculated as the linear regression of the seasonal timeseries of IASI and smoothed sonde LT columns in Dobson unit.

Atmospheric
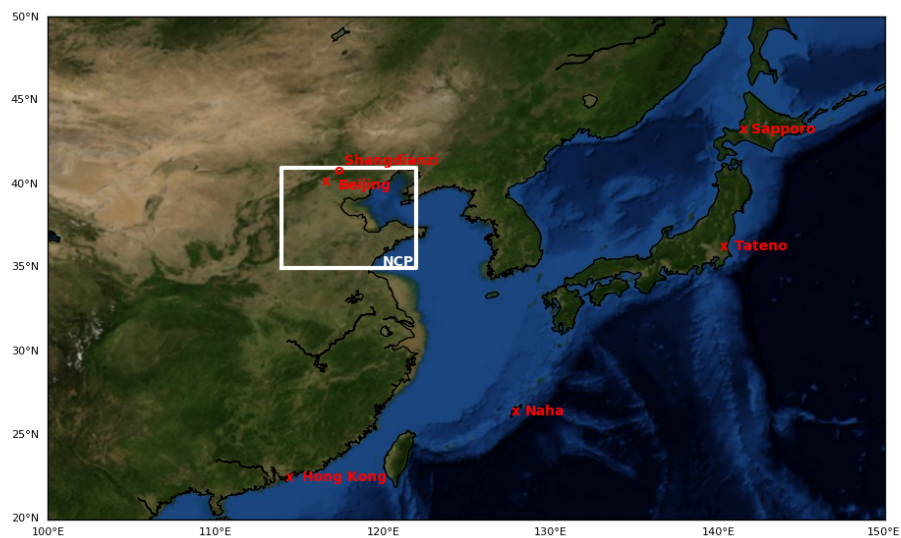Chemistry
and Physics
Discussions

Figure 1: Localization of the NCP region considered in the study indicated by the large square as well as the surface (o) and ozonesonde (x) stations.
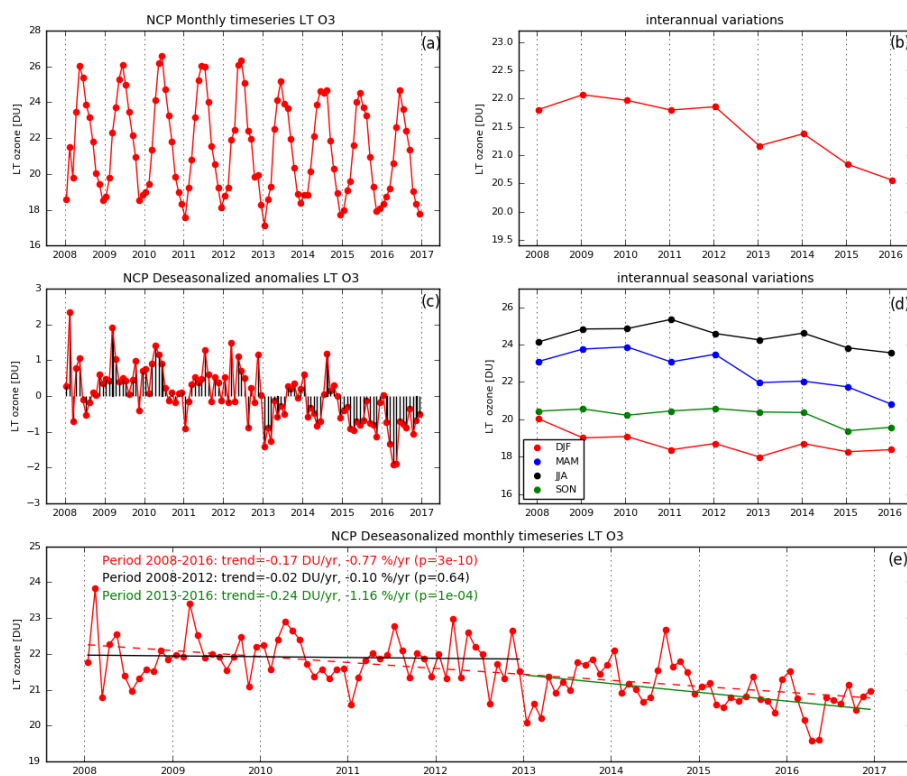
Atmospheric
Chemistry
and Physics
Discussions

Open Access

EGU

Figure 2: Monthly, annual and seasonal evolution of LT ozone over the NCP between 2008 and 2016 derieved from IASI-A. (a) monthly timeseries, (b) annual timeseries, (c) anomalies, (d) interannual variation of seasonal means, (e) deseasonalized monthly timeseries with linear regression calculated for the 2008-2016 period (red), the 2008-2012 period (black), and the 2013-2016 period (green).
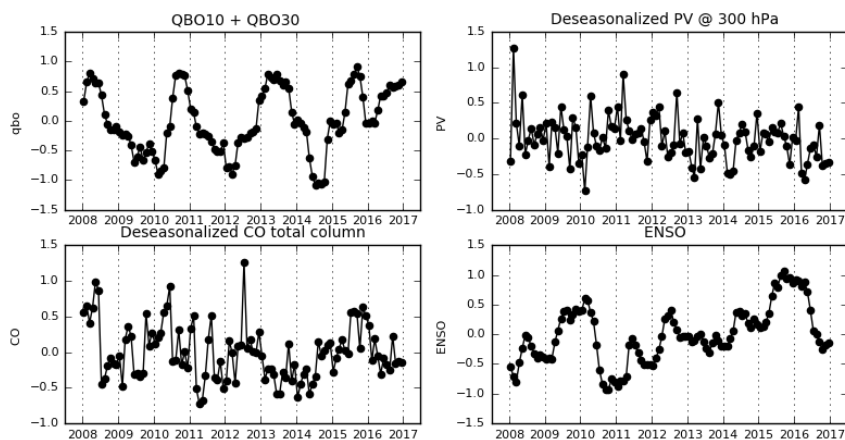
Figure 3: Normalized explanatory variable timeseries between 2008 and 2016.

Atmospheric
Chemistry
and Physics
Discussions
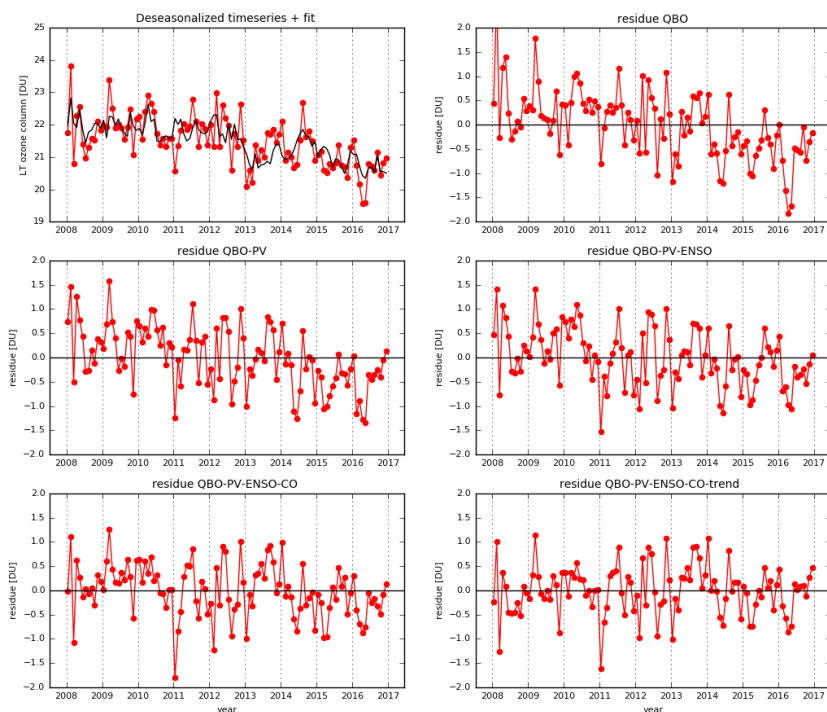
Figure 4: Deseaonalized monthly timeseries of LT ozone and the final fit result obtained with the regression model (top, left), and evolution of the residue when including the different explanatory variables. The right lower panel show the residual after all fits have been applied. It corresponds to the difference between the timeseries and the fit in the top left panel.
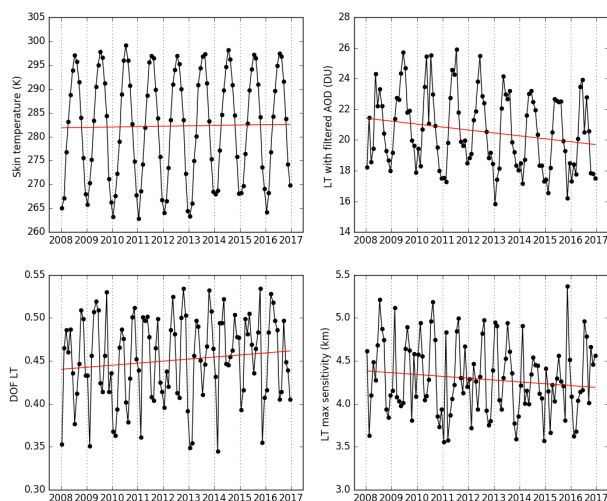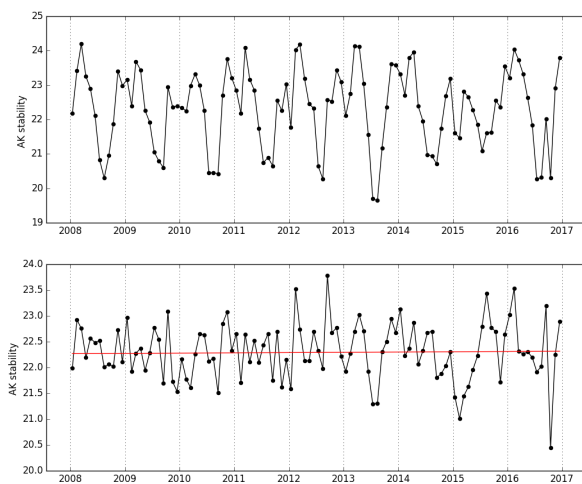
5

Atmospheric
Chemistry
and Physics
Discussions

Figure 5: Monthly timseries and their associated linear trends of different internal and external parameters used to test the retrieval stability.

5 **Figure 6: Monthly timeseries (top) and its associated deseasonalized timeseries and linear trend calculated for a unique ozone profile smoothed by each individual averaging kernel of IASI over the NCP between 2008 and 2016.**
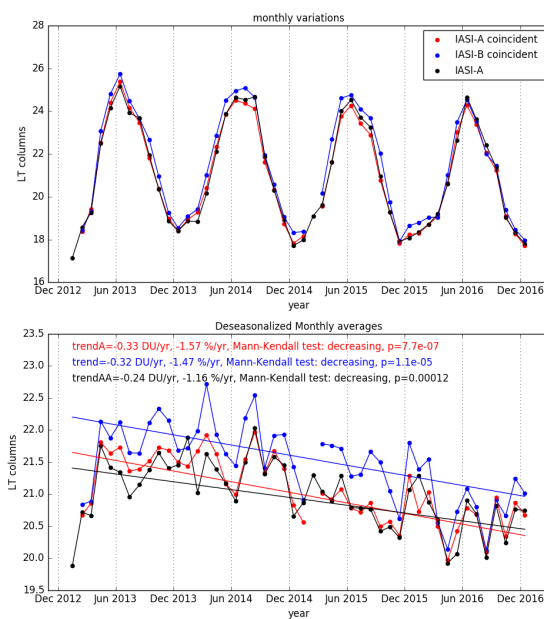
Figure 7: Monthly timeseries of IASI-A and IASI-B (blue). The IASI-A timeseries is plotted in red when in coincidence with IASI-B and in black when all IASI-A observations are considered. The deseasonnalized timeseries and the corresponding linear trends are given in the bottom panel.
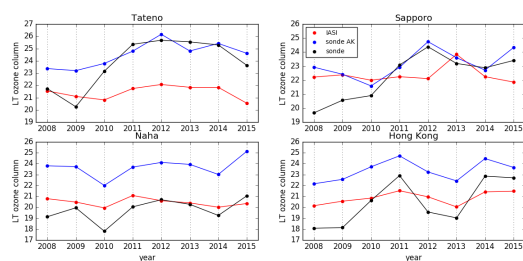

Figure 8: Interannual variations of LT ozone columns observed by IASI (red) and measured by sondes with (blue) and without (black) applying the averaging kernels for 4 Asian stations (Tateno, Sapporo, Naha, and Hong Kong).
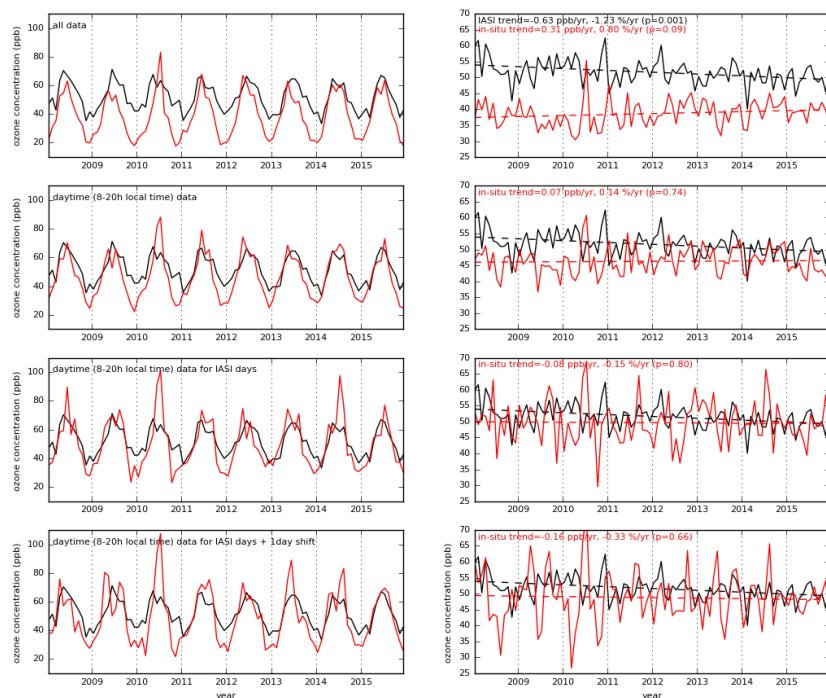
25

Figure 9: Evolution of the timeseries (deseasonalized or not) when changing the sampling. The IASI equivalent column concentrations are plotted in black, the surface concentrations measured at the Shangdianzi station, China, in red.